

## Equilibrium phases in the $\text{Bi}_2\text{O}_3\text{--TiO}_2\text{--WO}_3$ system

T. Jardiel<sup>a,\*</sup>, A.C. Caballero<sup>a</sup>, M. Villegas<sup>a</sup>, M. Valant<sup>b</sup>, B. Jancar<sup>b</sup>, D. Suvorov<sup>b</sup>

<sup>a</sup> *Electroceramics Department, Instituto de Cerámica y Vidrio-CSIC, 28049 Madrid, Spain*

<sup>b</sup> *Advanced Materials Department, Jožef Stefan Institute, 1000 Ljubljana, Slovenia*

Available online 10 March 2006

### Abstract

Phase relations in the  $\text{Bi}_2\text{O}_3\text{--TiO}_2\text{--WO}_3$  ternary system were evaluated for different compositions calcined in air at  $850^\circ\text{C}$  by means of XRD techniques. A solid solution area was observed for  $\text{Bi}_4\text{Ti}_3\text{O}_{12}$  compositions with a small amount of  $\text{WO}_3$ . The experimental results suggest the existence of a new phase with a nominal composition close to  $\text{Bi}_3\text{Ti}_{2.5}\text{W}_{0.5}\text{O}_{11}$ . This phase allows the definition of four triangles of compatibility at  $850^\circ\text{C}$  in the ternary system. The new phase was characterized by XRD, SEM and EDS.

© 2006 Elsevier Ltd. All rights reserved.

**Keywords:**  $\text{Bi}_4\text{Ti}_3\text{O}_{12}$  ceramics; Powders-solid state reaction; X-ray methods

### 1. Introduction

Fifty years ago, Aurivillius discovered the family of bismuth-based layer compounds; many groups have carried out crystallographic studies, and ferroelectric and piezoelectric properties have been found. Structurally, those compounds may be described as regular intergrowths of alternating perovskite-like and fluorite-like layers, with the general compositions  $[\text{A}_{m-1}\text{B}_m\text{O}_{3m+1}]^{2-}$  and  $[\text{Bi}_2\text{O}_2]^{2+}$ , respectively, where  $m$  is the number of the  $\text{BO}_6$  octahedra in the perovskite-like layer ( $m = 1, 2, 3, 4$  and  $5$ ). By changing the value of  $m$  in this sequence, a considerable number of compounds build up, all belonging to this family. Amongst these compositions, the most studied is the bismuth titanate,  $\text{Bi}_4\text{Ti}_3\text{O}_{12}$  (BIT), a high temperature ferroelectric ceramic ( $T_c = 675^\circ\text{C}$ )<sup>1</sup> with useful properties for an optical memory, piezoelectric and electro-optic devices.<sup>2,3</sup> In this material, however, the main component of the spontaneous polarization ( $P_s \approx 50 \mu\text{C}/\text{cm}$ ) lies in the  $ab$  plane<sup>3</sup> whereas the electrical conductivity is also very high in this plane<sup>4,5</sup> making it difficult to polarize. Such anisotropy is also reflected in the grain-growth habit. Typical microstructures of BIT-based ceramics show large platelet-like grains growing preferentially in the  $ab$  plane. As it has been shown, the aspect ratio of the platelets plays a critical role in the conductivity of BIT ceramics.<sup>6</sup>

Partial substitution of  $\text{Ti}^{4+}$  by a higher valence cation such as  $\text{W}^{6+}$  decreases the conductivity.<sup>7</sup> Furthermore, the effect of different doping routes with  $\text{W}^{6+}$  as donor cation has been studied from the point of view of its electrical behaviour but also of the structural and microstructural features. Doping with  $\text{WO}_3$  modifies the sintering behaviour and the grain-growth habit when compared with undoped BIT. The different microstructures obtained to a great extent determine the electrical properties of BIT-based materials.<sup>8</sup> In the case of BIT coprecipitated powders, the addition of small amounts of  $\text{WO}_3$  produce not only grain-growth control but also an increase of the maximum density at temperature up to  $850^\circ\text{C}$  for samples with 2–8 mol% of  $\text{WO}_3$ . This low temperature has been chosen for development in this study.<sup>9</sup>

However, the solid solution limit of the  $\text{WO}_3$  in BIT as well as the  $\text{Bi}_2\text{O}_3\text{--TiO}_2\text{--WO}_3$  phase diagram itself, remain unknown. If the solid solution limit is exceeded secondary phases appear in the material, which have a severe influence on the electric and ferroelectric properties.<sup>9</sup> In order to control the presence of these secondary phases in W-doped BIT ceramics, a preliminary study of the compatible phases in the  $\text{Bi}_2\text{O}_3\text{--TiO}_2\text{--WO}_3$  system in the vicinity of  $\text{Bi}_4\text{Ti}_3\text{O}_{12}$  region at  $850^\circ\text{C}$  is presented.

### 2. Experimental procedure

Twenty different compositions were prepared in the ternary system  $\text{Bi}_2\text{O}_3\text{--TiO}_2\text{--WO}_3$  (Table 1). Samples were prepared by solid state reaction using high purity  $\text{Bi}_2\text{O}_3$ ,  $\text{TiO}_2$  and  $\text{WO}_3$  (99.99%) raw materials. The powders were mixed in a ball mill

\* Corresponding author. Tel.: +34 917355840; fax: +34 917355843.  
E-mail address: [jardiel@icv.csic.es](mailto:jardiel@icv.csic.es) (T. Jardiel).

Table 1  
Compositions prepared in the  $\text{Bi}_2\text{O}_3$ – $\text{TiO}_2$ – $\text{WO}_3$  system

	Label	Composition (mol%)		
		$\text{Bi}_2\text{O}_3$	$\text{TiO}_2$	$\text{WO}_3$
$\text{Bi}_4\text{Ti}_3\text{O}_{12} + \text{WO}_3$	(1)	40.00	60.00	0.00
	(2)	39.25	58.75	2.00
	(3)	38.15	56.85	5.00
	(4)	37.00	55.00	8.00
	(5)	34.00	51.00	15.00
$\text{Bi}_2\text{Ti}_2\text{O}_7 + \text{WO}_3$	(6)	33.33	66.66	0.00
	(7)	32.50	65.50	2.00
	(8)	31.25	63.75	5.00
	(9)	30.25	61.75	8.00
	(10)	28.00	57.00	15.00
$\text{Bi}_2\text{Ti}_4\text{O}_{11} + \text{WO}_3$	(11)	20.00	80.00	0.00
	(12)	19.25	78.75	2.00
	(13)	18.75	76.25	5.00
	(14)	18.50	73.50	8.00
	(15)	17.00	68.00	15.00
$\text{Bi}_4\text{Ti}_3\text{O}_{12} + \text{Bi}_6\text{Ti}_3\text{WO}_{18}$	(16)	32.50	65.50	2.00
	(17)	41.00	54.00	5.00
	(18)	41.50	50.50	8.00
	(19)	42.86	42.86	14.28

with  $\text{ZrO}_2$  balls and ethanol and then dried at  $80^\circ\text{C}$  and uniaxially pressed into pellets. The pellets were first calcined at  $750^\circ\text{C}$  for 10 h, crushed, mixed in agate mortar, uniaxially pressed to achieve homogeneity and then calcined again at  $850^\circ\text{C}$  for 10 h.

The phases present in the calcined specimens were determined by X-ray diffraction (XRD, Siemens D5000, Cu  $K\alpha$  radiation, step 0.02). The microstructures of the compacts were studied by scanning electron microscopy (SEM, Carl Zeiss DSM 950) equipped with energy dispersive spectroscopy (EDS) on polished and chemically etched surfaces.

### 3. Results and discussion

The binary systems  $\text{Bi}_2\text{O}_3$ – $\text{TiO}_2$ ,<sup>10,11</sup>  $\text{Bi}_2\text{O}_3$ – $\text{WO}_3$ ,<sup>12</sup>  $\text{TiO}_2$ – $\text{WO}_3$ <sup>13</sup> are described in the literature. The  $\text{Bi}_6\text{Ti}_3\text{WO}_{18}$ <sup>14</sup> and  $\text{Bi}_{10}\text{Ti}_3\text{W}_3\text{O}_{30}$ <sup>15</sup> phases have been studied by different authors. The experimental compositions prepared in the ternary system are marked with black circles in Fig. 1. A more accurate description is now provided.

#### 3.1. $\text{Bi}_4\text{Ti}_3\text{O}_{12}$ – $\text{Bi}_6\text{Ti}_3\text{WO}_{18}$ line

XRD diffraction patterns of samples 1, 17, 18 and 19 are shown in Fig. 2. Samples located on the join line between  $\text{Bi}_4\text{Ti}_3\text{O}_{12}$  and  $\text{Bi}_6\text{Ti}_3\text{WO}_{18}$  phases are actually a mixture of these two phases.

#### 3.2. $\text{Bi}_4\text{Ti}_3\text{O}_{12}$ – $\text{Bi}_2\text{Ti}_4\text{O}_{11}$ – $\text{Bi}_6\text{Ti}_3\text{WO}_{18}$ triangle

XRD spectra of samples 7 and 8 (Fig. 3) show a mixture of three phases  $\text{Bi}_4\text{Ti}_3\text{O}_{12}$ ,  $\text{Bi}_2\text{Ti}_4\text{O}_{11}$  and  $\text{Bi}_6\text{Ti}_3\text{WO}_{18}$  defining an area of compatibility for these three compounds. The  $\text{Bi}_2\text{Ti}_2\text{O}_7$  phase (6) reported by Masuda et al.<sup>16</sup> is not stable at  $850^\circ\text{C}$ . The

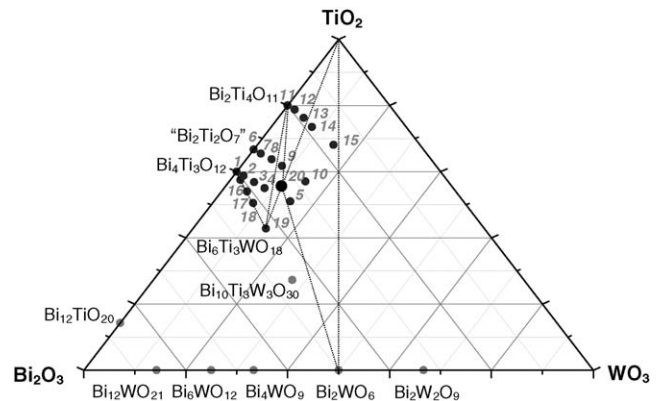


Fig. 1. Ternary diagram, showing triangles of compatibility, for the  $\text{Bi}_2\text{O}_3$ – $\text{TiO}_2$ – $\text{WO}_3$  system at  $850^\circ\text{C}$  in air.

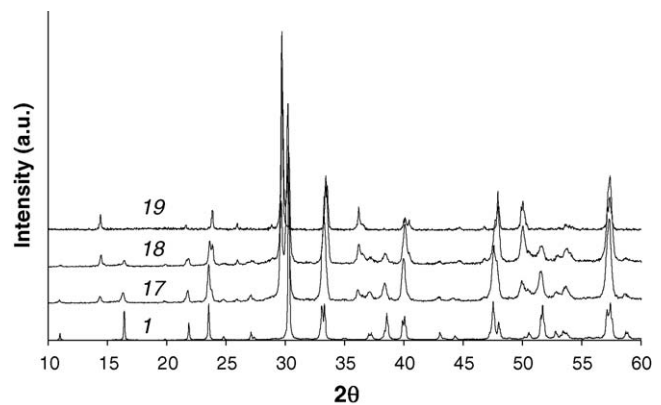


Fig. 2. XRD diffractogram for: sample 1 that corresponds to  $\text{Bi}_4\text{Ti}_3\text{O}_{12}$ , sample 19 that corresponds to  $\text{Bi}_6\text{Ti}_3\text{WO}_{18}$  and samples 17 and 18 that represent a mixture of both phases.

XRD patterns of the samples 2, 3 and 4 on the  $\text{Bi}_4\text{Ti}_3\text{O}_{12}$ – $\text{WO}_3$  join line (Fig. 4), show only one  $\text{Bi}_4\text{Ti}_3\text{O}_{12}$  phase, showing that these samples are actually located in a solid solution area. The observed slight displacement of the XRD pattern in these samples with regard to that of pure  $\text{Bi}_4\text{Ti}_3\text{O}_{12}$  is due to a change in the lattice parameters associated with the incorporation of  $\text{W}^{6+}$  into BIT lattice.

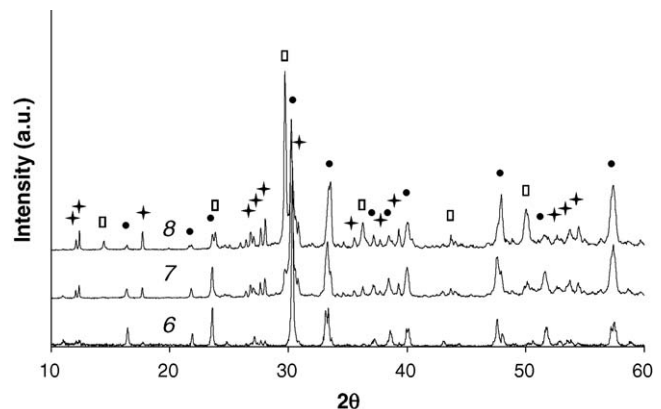


Fig. 3. XRD diffractogram for: samples 6, 7 and 8. (+)  $\text{Bi}_2\text{Ti}_4\text{O}_{11}$ ; (□)  $\text{Bi}_6\text{Ti}_3\text{WO}_{18}$ ; (●)  $\text{Bi}_4\text{Ti}_3\text{O}_{12}$ .

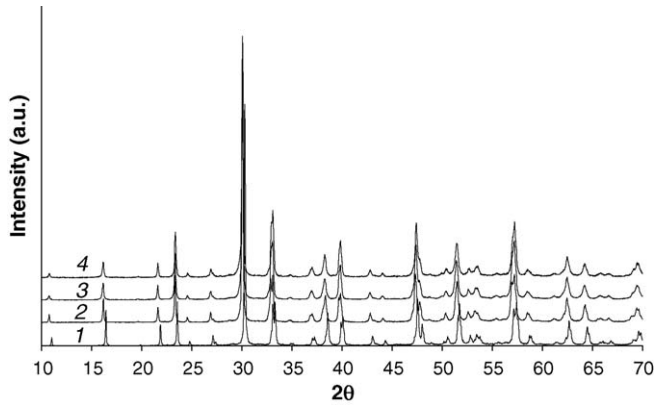


Fig. 4. XRD diffractogram for samples 1, 2, 3 and 4. All the peaks correspond to the  $\text{Bi}_4\text{Ti}_3\text{O}_{12}$  phase.

### 3.3. $\text{Bi}_2\text{Ti}_4\text{O}_{11}$ – $\text{Bi}_6\text{Ti}_3\text{WO}_{18}$ – $\text{WO}_3$ triangle

XRD diffraction patterns of samples 10 and 15 (Fig. 5) show a mixture of two phases,  $\text{Bi}_2\text{WO}_6$  and  $\text{TiO}_2$ , together with a group of peaks that cannot be assigned to any known phase in this system. The same peaks are observed in XRD spectra of sample 9, together with  $\text{Bi}_2\text{Ti}_4\text{O}_{11}$  and  $\text{Bi}_6\text{Ti}_3\text{WO}_{18}$  phases (Fig. 6), and also in those XRD diffraction patterns of samples 12 and 13 in addition to  $\text{Bi}_2\text{Ti}_4\text{O}_{11}$  and  $\text{TiO}_2$  peaks (Fig. 7).

Two different compounds exhibit an XRD pattern that completely fits that group of unidentified peaks,  $\text{Bi}_3(\text{AlSb}_2)\text{O}_{11}$ <sup>17</sup> (JCPDS no. 86-1537) and  $\text{PbHoAl}_3\text{O}_8$ <sup>18</sup> (JCPDS no. 80-0046), both with cubic symmetry and structures comprising two interpenetrating networks of  $(\text{AlSb}_2)\text{O}_9$  or  $\text{Al}_3\text{O}_9$  arrays of pairs of edge-sharing octahedra and a array of corner-sharing  $\text{Bi}_8\text{O}_4$  or  $\text{Pb}_4\text{LnO}_7$  linked tetrahedra. This indicates that the unknown group of peaks could correspond to just one phase with a similar structure to these. SEM analysis confirms this assumption; the SEM micrograph of sample 15 clearly shows the existence of three phases in the microstructure of the ceramic (Fig. 8). EDS analysis of these phases allowed the identification of  $\text{TiO}_2$  and  $\text{Bi}_2\text{WO}_6$  phases. However, the Bi/Ti/W ratio of the third phase (Table 2) did not fit to any known composition in the system

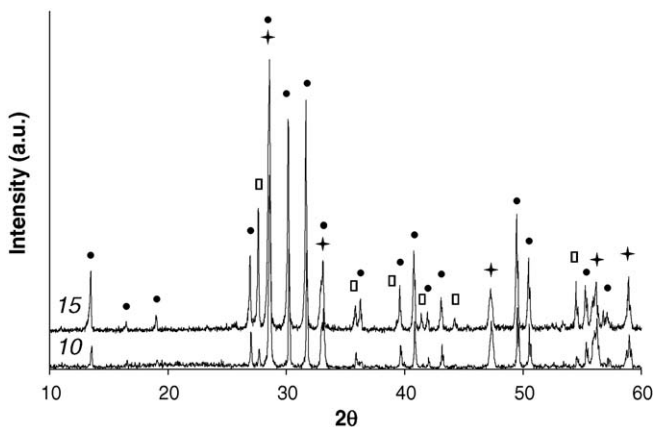


Fig. 5. XRD diffractogram for samples 10 and 15. (+)  $\text{Bi}_2\text{WO}_6$ ; (□)  $\text{TiO}_2$ ; (●) new phase.

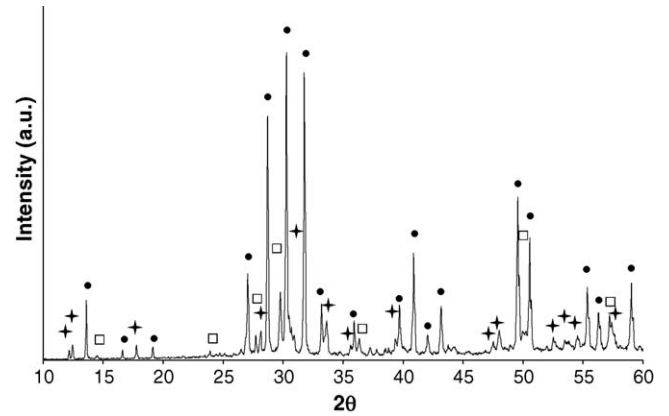


Fig. 6. XRD diffractogram for sample 9. (+)  $\text{Bi}_2\text{Ti}_4\text{O}_{11}$ ; (□)  $\text{Bi}_6\text{Ti}_3\text{WO}_{18}$ ; (●) new phase.

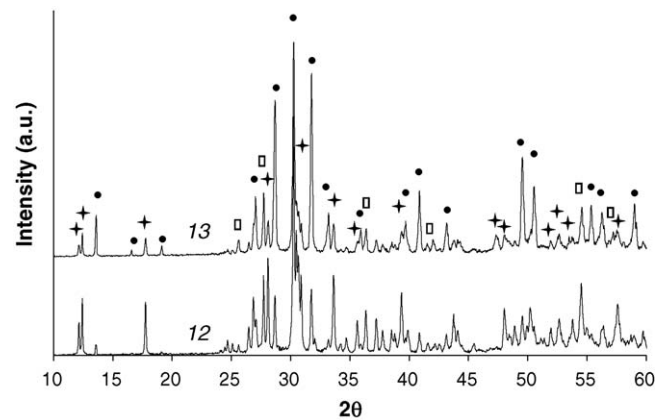


Fig. 7. XRD diffractogram for samples 12 and 13. (+)  $\text{Bi}_2\text{Ti}_4\text{O}_{11}$ ; (□)  $\text{TiO}_2$ ; (●) new phase.

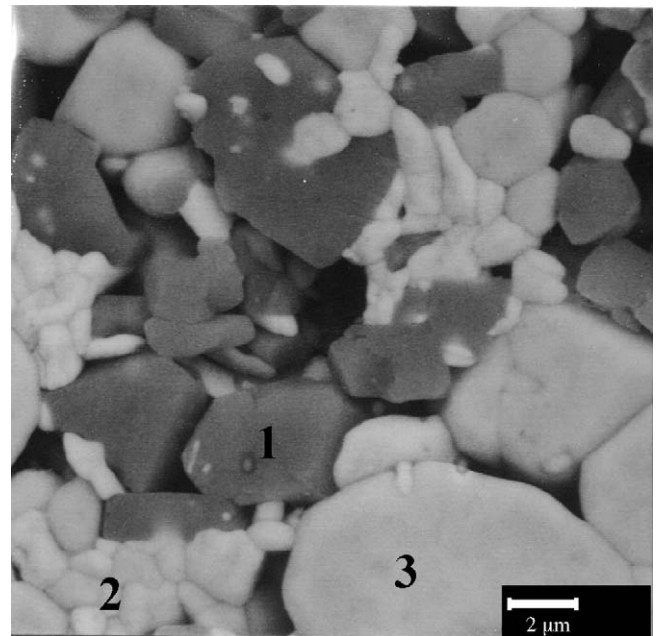


Fig. 8. SEM micrograph of sample 15 (polished and chemically etched surface). It is possible to recognize three different phases: (1)  $\text{TiO}_2$ ; (2)  $\text{Bi}_2\text{WO}_6$ ; and (3) a new phase.

Table 2  
EDS analysis of the unknown phase

Element	Net counts	Weight conc. (%)	Atom conc. (%)	Compound conc. (%)	Formula
O	0	17.06	64.34	0.00	–
Ti	2096	11.79	14.85	19.66	TiO <sub>2</sub>
W	338	6.96	2.29	8.78	WO <sub>3</sub>
Bi	797	64.18	18.53	71.55	Bi <sub>2</sub> O <sub>3</sub>

Bi<sub>2</sub>O<sub>3</sub>–TiO<sub>2</sub>–WO<sub>3</sub>. Taking into account the crystal structures of the Bi<sub>3</sub>(AlSb<sub>2</sub>)O<sub>11</sub> and PbHoAl<sub>3</sub>O<sub>8</sub> phases which exhibit a similar XRD pattern and the Bi<sub>2</sub>O<sub>3</sub>–TiO<sub>2</sub>–WO<sub>3</sub> ratio of the new phase, a preliminary composition for this third phase can be proposed as: Bi<sub>3</sub>Ti<sub>2.5</sub>W<sub>0.5</sub>O<sub>11</sub> (20).

When locating this new composition in the Bi<sub>2</sub>O<sub>3</sub>–TiO<sub>2</sub>–WO<sub>3</sub> phase diagram, it is then possible to establish at least three new triangles of compatibility: Bi<sub>2</sub>Ti<sub>4</sub>O<sub>11</sub>–TiO<sub>2</sub>–Bi<sub>3</sub>Ti<sub>2.5</sub>W<sub>0.5</sub>O<sub>11</sub>, Bi<sub>2</sub>Ti<sub>4</sub>O<sub>11</sub>–Bi<sub>6</sub>Ti<sub>3</sub>WO<sub>18</sub>–Bi<sub>3</sub>Ti<sub>2.5</sub>W<sub>0.5</sub>O<sub>11</sub> and Bi<sub>2</sub>WO<sub>6</sub>–TiO<sub>2</sub>–Bi<sub>3</sub>Ti<sub>2.5</sub>W<sub>0.5</sub>O<sub>11</sub>.

### 3.4. Description of the new Bi<sub>3</sub>Ti<sub>2.5</sub>W<sub>0.5</sub>O<sub>11</sub> phase

On the basis of the determined molar ratio, the new phase was prepared by the same processing method as that for the other compositions, but this time with an additional calcination step at 1000 °C for 60 h. Fig. 9 shows the XRD diffraction pattern obtained for this composition. It can be seen that a small amount of the Bi<sub>10</sub>Ti<sub>3</sub>W<sub>3</sub>O<sub>30</sub> phase is also present in the spectra. This fact may indicate that the suggested composition does not fit exactly the Bi<sub>3</sub>Ti<sub>2.5</sub>W<sub>0.5</sub>O<sub>11</sub> formula so slight changes need to be made. However, it is necessary to take into account that partial decomposition of the new phase at 1000 °C could have occurred. The lattice parameters were calculated for the peaks corresponding to the new phase. These correspond to cubic symmetry:  $a = b = c = 9.4196 \pm 0.0001$  Å. These values are quite similar to the parameters observed for the analogous structures.

Fig. 10 shows an SEM micrograph for the new sample sintered at 1000 °C for 10 h. Pellets were polished and chemically etched.<sup>19</sup> Rounded grains are observed with an average grain size approximately 5 μm and a high level of porosity. The

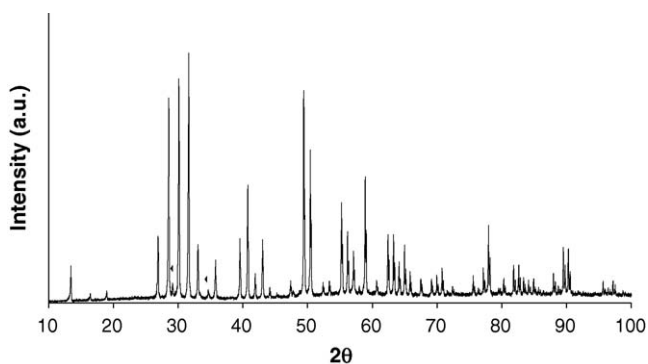


Fig. 9. XRD diffractogram for the Bi<sub>3</sub>Ti<sub>2.5</sub>W<sub>0.5</sub>O<sub>11</sub> phase. All the peaks correspond to this phase except marked peaks that possibly correspond to Bi<sub>10</sub>Ti<sub>3</sub>W<sub>3</sub>O<sub>30</sub> phase.

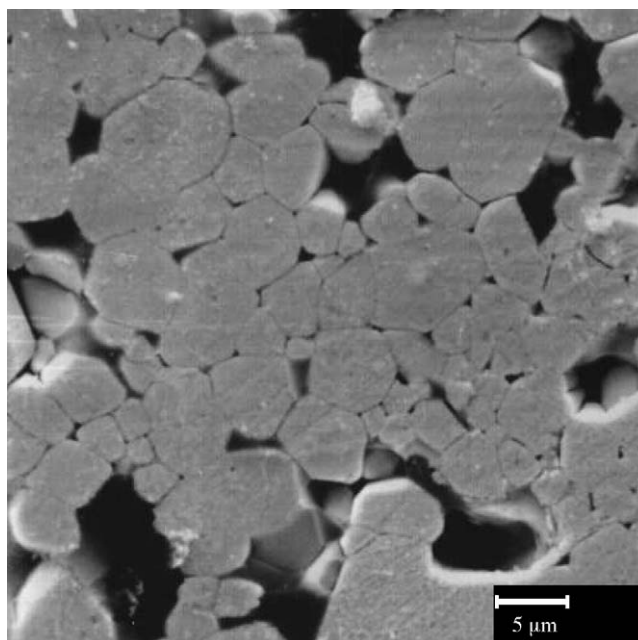


Fig. 10. SEM micrograph of sample 20 (polished and chemically etched surface).

homogeneity of the sample was verified using EDS analysis; it confirmed the expected bulk composition. It must be noted that EDS analysis is limited in the degree of precision it can provide.

## 4. Conclusions

A new stable phase with composition close to Bi<sub>3</sub>Ti<sub>2.5</sub>W<sub>0.5</sub>O<sub>11</sub> was found and as a result four triangles of compatibility have been established in the Bi<sub>2</sub>O<sub>3</sub>–TiO<sub>2</sub>–WO<sub>3</sub> system: Bi<sub>4</sub>Ti<sub>3</sub>O<sub>12</sub>–Bi<sub>2</sub>Ti<sub>4</sub>O<sub>11</sub>–Bi<sub>6</sub>Ti<sub>3</sub>WO<sub>18</sub>, Bi<sub>2</sub>Ti<sub>4</sub>O<sub>11</sub>–TiO<sub>2</sub>–Bi<sub>3</sub>Ti<sub>2.5</sub>W<sub>0.5</sub>O<sub>11</sub>, Bi<sub>2</sub>Ti<sub>4</sub>O<sub>11</sub>–Bi<sub>6</sub>Ti<sub>3</sub>WO<sub>18</sub>–Bi<sub>3</sub>Ti<sub>2.5</sub>W<sub>0.5</sub>O<sub>11</sub> and Bi<sub>2</sub>WO<sub>6</sub>–TiO<sub>2</sub>–Bi<sub>3</sub>Ti<sub>2.5</sub>W<sub>0.5</sub>O<sub>11</sub>. For WO<sub>3</sub> levels below 8 mol%, a solid solution region is constituted by the phases Bi<sub>4</sub>Ti<sub>3</sub>O<sub>12</sub> and WO<sub>3</sub>.

## Acknowledgements

The authors want to express their gratitude to the “Comisión Interministerial de Ciencia y Tecnología” (CICYT), project MAT2004-04843-C02-01 and to the “Ministerio de Educación y Ciencia”, MEC-FPI fellowship program, for the support of this work.

## References

1. Aurivillius, B., Mixed bismuth oxides with layer lattices. *Ark. Kemi.*, 1949, **1**, 463–480.
2. Dorrian, J. F., Newnham, R. E. and Smith, D. K., Crystal structure of Bi<sub>4</sub>Ti<sub>3</sub>O<sub>12</sub>. *Ferroelectrics*, 1971, **3**, 17–21.
3. Cummings, S. E. and Cross, L. E., Electrical and optical properties of ferroelectric Bi<sub>4</sub>Ti<sub>3</sub>O<sub>12</sub> single crystals. *J. Appl. Phys.*, 1968, **39**, 2268–2274.
4. Fouskova, A. and Cross, L. E., Dielectric properties of bismuth titanate. *J. Appl. Phys.*, 1970, **41**, 2834–2838.

5. Takenaka, T. and Sakata, K., Grain orientation effects and electrical properties of bismuth layer structured ferroelectric  $\text{Pb}_{1-x}(\text{Na/Ce})_x\text{Bi}_4\text{Ti}_4\text{O}_{15}$  solid solution. *J. Appl. Phys.*, 1984, **55**, 1092.
6. Villegas, M., Caballero, A. C., Moure, C., Durán, P. and Fernández, J. F., Factors affecting the electrical conductivity of donor-doped  $\text{Bi}_4\text{Ti}_3\text{O}_{12}$  piezoelectric ceramics. *J. Am. Ceram. Soc.*, 1999, **82**, 2411–2416.
7. Lopatin, S. S., Lupeiko, T. G., Vasil'tsova, T. L., Basenko, N. I. and Berlizev, I. M., Properties of bismuth titanate ceramic modified with group VI elements. *Izvestiya Akademii Nauk SSSR, Neorganicheskie Materialy*, 1989, **24**(9), 1551–1554.
8. Villegas, M., Caballero, A. C. and Fernández, J. F., Modulation of electrical conductivity through microstructural control in  $\text{Bi}_4\text{Ti}_3\text{O}_{12}$ -based piezoelectric ceramics. *Ferroelectrics*, 2002, **267**, 165–173.
9. Villegas, M., Jardiel, T., Caballero, A. C. and Fernández, J. F., Electrical properties of bismuth titanate based ceramics with secondary phases. *J. Electroceram.*, 2004, **13**(1–3), 543–548.
10. Speranskaya, E. I., Rez, I. S., Kozlova, L. V., Skorikov, V. M. and Slavov, V. I., The system bismuth oxide–titanium oxide. *J. Inorg. Mater. (English Translation)*, 1965, **213**.
11. Miyazawa, S. and Tabata, T.,  $\text{Bi}_2\text{O}_3$ – $\text{TiO}_2$  binary phase diagram study for TSSG pulling of  $\text{Bi}_{12}\text{TiO}_{20}$  single crystals. *J. Cryst. Growth*, 1998, **191**(3), 512–516.
12. Speranskaya, E. I., The  $\text{Bi}_2\text{O}_3$ – $\text{WO}_3$  system. *Inorg. Mater.*, 1970, **6**(1), 127–129.
13. Chang, L. L. Y., Scroger, M. G. and Phillips, B., High-temperature condensed-phase equilibria in system Ti–W–O. *J. Less-Common Metals*, 1967, **12**(1), 51–56.
14. Hyatt, N. C., Reaney, I. M. and Knight, K. S., Ferroelectric-paraelectric phase transition in the  $n=2$  Aurivillius phase  $\text{Bi}_3\text{Ti}_{15}\text{W}_{0.5}\text{O}_9$ : A neutron powder diffraction study. *Phys. Rev. B*, 2005, **71**(2), p. 024119.
15. Shebanov, L. A., Osipyan, V. G., Freidenfeld, E. Z. and Birks, E. H., Ferroelectricity in  $\text{Bi}_{10}\text{Ti}_3\text{W}_3\text{O}_{30}$ . *Physica Status Solidi A—Appl. Res.*, 1982, **71**(1), K61–K62.
16. Masuda, Y., Masumoto, H., Baba, A., Goto, T. and Iría, T., Crystal growth, dielectric and polarization reversal properties of  $\text{Bi}_4\text{Ti}_3\text{O}_{12}$  single crystal. *Jpn. J. Appl. Phys., Part 1*, 1992, **31**(9B), 3108–3112.
17. Ismunandar, B. J., Kennedy, B. A. and Hunter, Structural and surface properties of  $\text{Bi}_3(\text{MSb}_2)\text{O}_{11}$  ( $M=\text{Al}, \text{Ga}$ ). *J. Solid State Chem.*, 1996, **127**(2), 178–185.
18. Scheikowski, M. and Müller-Buschbaum, H. K., Crystal-chemistry of the lead lanthanide oxoaluminates—on  $\text{Pb}_2\text{HoAl}_3\text{O}_8$  and  $\text{Pb}_2\text{LuAl}_3\text{O}_8$ . *Z. Anorg. Allg. Chem.*, 1993, **619**(10), 1755–1758.
19. Jardiel, T., Caballero, A.C., Villegas, M., Chemical etching of  $\text{Bi}_4\text{Ti}_3\text{O}_{12}$  ceramics. *J. Eur. Ceram. Soc.*, in press.